International Journal of Pharmaceutics 393 (2010) 119–126

Contents lists available at ScienceDirect

International Journal of Pharmaceutics

journal homepage: www.elsevier.com/locate/ijpharm

Co-delivery of doxorubicin and plasmid by a novel FGFR-mediated cationic liposome

Wenjing Xiao[a,b], Xiang Chen[a], Li Yang[a], Yongqiu Mao[a], Yuquan Wei[a], Lijuan Chen[a,b,*]

[a] State Key Laboratory of Biotherapy, West China Hospital, West China Medical School, Sichuan University, Chengdu 610041, China
[b] West China School of Pharmacy, West China Medical School, Sichuan University, Chengdu, China

ARTICLE INFO

Article history:
Received 21 September 2009
Received in revised form 14 April 2010
Accepted 15 April 2010
Available online 21 April 2010

Keywords:
Cationic liposomes
Doxorubicin
Plasmid
FGF-mediated

ABSTRACT

In our previous study, we developed a novel cationic liposome, which was modified with truncated human basic fibroblast growth factor (tbFGF) peptide. This tbFGF-mediated cationic liposome could deliver chemotherapeutic agents or gene specifically to FGFRs on tumors and obtained higher transfection efficiency than plain cationic liposomes. In order to investigate whether this novel cationic liposome could achieve a synergistic/combined anti-tumor effect as a co-delivery system, we simultaneously delivered doxorubicin (DOX) and the plasmid encoding the phosphorylation-defective mouse survivin threonine 34 → alanine mutant (Msurvivin T34A plasmid) to the same cells through this cationic liposome. As a result, an enhanced antiproliferative activity *in vitro* has been achieved by delivering DOX and DNA simultaneously to the Lewis lung carcinoma cells (LLC) using this liposome. The concentration of DOX in the co-delivery system which caused 50% killing was nearly 3-fold lower than that of the free DOX. Furthermore, the co-delivery system suppressed tumor growth more efficiently than either DOX or the Msurvivin T34A plasmid alone in the Lewis lung carcinoma-bearing C57BL/6 mice. After 18 days of treatment with the co-delivery system, the average tumor volume in mice was decreased by 80%, which was higher than liposomal DOX (70%, $P < 0.05$) and Msurvivin T34A plasmid (41%, $P < 0.01$). The co-delivery system also caused 15 days delay of tumor growth, which was longer than the other treatment groups. In conclusion, this novel cationic liposome is an efficient vector to simultaneously deliver drugs and DNA to the same cells *in vitro* and *in vivo*.

1. Introduction

Co-delivery system, which could deliver drugs and DNA simultaneously to the same cells *in vitro* and *in vivo* has been proposed to enhance gene expression or achieve the synergistic/combined effect of drug and gene therapies (Zhang et al., 2001; Kishida et al., 2003; Janát-Amsbury et al., 2004). Some studies suggested that cationic liposome could be used as a successful co-delivery system to deliver DNA and drugs into the immune cells (Liu et al., 2004). Meanwhile these liposomes have been demonstrated significant benefits as delivery systems for anticancer drugs because of their selectively targeting angiogenic endothelial cells in tumors (Thurston et al., 1998). In addition, as non-viral vectors, they could be safely administered to humans for their lower toxicity and immunogenicity than viral vectors (Xu et al., 1997).

However, the obstacle of the cationic liposome used as a vector for DNA was the low transfection efficiency in contrast to viral vectors (Nakase et al., 2005). Numerous strategies have been explored to overcome this disadvantage including receptor-mediated gene delivery methods (Hara et al., 1995). Basic fibroblast growth factor (FGF2)-receptor was reported to be ubiquitously up-regulated in many human tumor types, such as lung cancers (Takanami et al., 1996; Volm et al., 1997), making this receptor as an attractive target for cancer gene therapy. In fact, the FGF2-retargeted adenoviral (FGF2-Ad) molecular conjugates have been reported to obtain efficient transfer in many kinds of cells (Rogers et al., 1997; Rancourt et al., 1998; Gu et al., 1999; Printz et al., 2000; Kleeff et al., 2002). Moreover, our lab has reported the cationic liposome combining the truncated basic fibroblast growth factor (tbFGF) peptide (a.a. 30–115) can specifically lead to location in tumors (Chen et al., 2010). This peptide, containing FGF2-receptor binding site and part of heparin-binding site, could effectively bind FGF2-receptor on cell's surface, but not stimulate cell proliferation.

The aim of this paper was to evaluate the potential of the above-mentioned novel cationic liposome designed by our lab as a carrier to deliver drugs and DNA simultaneously in the same cells. Doxorubicin (DOX) and the plasmid encoding the

* Corresponding author at: State Key Laboratory of Biotherapy, West China Hospital, West China Medical School, Sichuan University, Gaopeng Street, Keyuan Road 4, Chengdu 610041, China. Tel.: +86 28 85164063, fax: +86 28 85164060.
E-mail addresses: lijuan17@hotmail.com, abbyxiao@hotmail.com, wx.satellitely@gmail.com (L. Chen).

0378-5173/$ – see front matter © 2010 Elsevier B.V. All rights reserved.
doi:10.1016/j.ijpharm.2010.04.018

phosphorylation-defective mouse survivin threonine 34 → alanine mutant (Msurvivin T34A plasmid), as the model drug and plasmid, were delivered to the same cells by it.

DOX, as an anthracycline antibiotic, has become part of standard treatment regiments for both hematological malignancies and solid tumors (Tan et al., 1973). However, it has been limited in clinical use for lack of tumor specificity and development of natural or acquired resistance to tumor (Zou et al., 1994). Many attempts have been done to overcome these limitations. Prodrug and particulate methods involved as active fields of DOX research for past two decades (Van Heeswijk et al., 1984). Liposomes also have been used as carriers for delivery of DOX to reduce side effect, such as anthracycline-induced cardiomyopathy (Batist et al., 2001). However, the clinical trails showed drug resistance even could not be solved by combination chemotherapy (Henk et al., 2009).

Survivin is an unique member of the inhibitor of apoptosis gene family, which is a M_r 16,500 intracellular protein (Salvesen and Duckett, 2002). Previous studies have demonstrated that the level of survivin protein appeared to be involved in tumor cell resistance to ionizing, radiation (Asanuma et al., 2000) and some chemotherapeutical drug, like DOX (Paduano et al., 2006). Thus, many attempts have been made to counteract survivin in tumor cells including anti-sense, ribozymes, RNAi-mediated survivin knockdown, survivin-directed vaccines or dominant negative mutants (Peng et al., 2008). Msurvivin T34A plasmid, as a dominant negative mutant has also been reported to reduce tumor cell proliferative potential and lead to caspase-dependent apoptosis in melanoma cell lines (Grossman et al., 2001; Kanwar et al., 2001).

Therefore, we supposed that this novel cationic liposome was an effective vector to deliver DOX to cells simultaneously with Msurvivin T34A plasmid, resulting in achieving the synergistic/combined anti-tumor effect *in vitro* and *in vivo* for the interaction of DOX with Msurvivin T34A plasmid.

2. Materials and methods

2.1. Materials

1,2-Dioleoyloxy-3-trimethylammonium-propane (DOTAP; Avanti Polar Lipids Inc., Alabaster, AL) and cholesterol (Chol; Sigma Chemical Co., St. Louis, MO) were used for preparation of the liposome. Pure doxorubicin (DOX; Meiji Seika Kaisha Ltd., Kitakami Plant) was used for encapsulation into cationic liposomes. The plasmid encoding the phosphorylation-defective mouse survivin threonine 34 → alanine mutant (Msurvivin T34A plasmid) and truncated human basic fibroblast growth factor (tbFGF) peptide were bound to the surface of cationic liposomes, prepared by our lab. A pEGFP-N1 plasmid designed for eukaryotic cell expression of the green fluorescent protein (GFP) was obtained from Elim Biopharmaceuticals (Hayward, CA).

2.2. Cells and culture conditions

LLC were incubated in DMEM (GIBICO). These cells were supplemented with 10% heat-inactivated fetal calf serum, 100 units/ml penicillin, 100 units/ml streptomycin, at 37 °C, 95% relative humidity, under 5% CO_2. Cell concentrations were determined by counting trypsinized cells with a hemocytometer.

2.3. Preparation of liposomes

Cationic liposomes (LPs) composed of DOTAP/Chol (molar ratio, 1:1) as described previously (Chen et al., 2010). Briefly, DOTAP and Chol were dissolved in chloroform. Then the mixture was warmed to 37 °C in a round-bottomed flask, and the solvent was evaporated under vacuum in a rotary evaporator until a thin lipid film was formed. Solvent traces were eliminated by drying the film at 5 millibars overnight. Lipid films were hydrated with 5% glucose (w/v) to achieve a final concentration of 5 mg/ml lipid. The hydrated lipid film was rotated in a water bath at 55 °C for 45 min to form multilamellar liposomes (MLVs), spontaneously. Then the MLVs were sonicated at 55 °C (200W, 5 min). Next, the suspension was extruded 3 times through polycarbonate membrane (Millipore Billerica, MA) with the size of 220 nm.

DOX was encapsulated in the LPs (LPs–DOX) using the transmembrane pH gradient loading procedure. 5 mg/ml of the LPs were mixed with 1 mg/ml DOX with equal volume at 55 °C for 15 min. tbFGF was combined to the LPs (tbFGF–LPs) and LPs–DOX (tbFGF–LPs–DOX) by incubated with respective liposomes at 4 °C overnight. The final LPs/tbFGF ratio is 12.5:1 (w:w). Msurvivin T34A plasmid, as the tbFGF, was also bound to the surface of liposomes. tbFGF–LPs–MsurvivinT34A and tbFGF–LPs–DOX–MsurvivinT34A were prepared by incubating Msurvivin T34A plasmid with tbFGF–LPs or tbFGF–LPs–DOX at 4 °C for 40 min to obtain the concentration of 0.05 mg/ml.

2.4. Characterization of liposomes

The particle size and surface charge of liposomes were analyzed, using Nano-ZS (Malvern Instruments, Herrenberg, Germany) at 25 °C (Ghera et al., 2009).

2.5. Transfection in vitro

Cells (LLC) grown to 60–70% confluence in 6-well plates were incubated in serum-free medium with LPs–pEGFP, tbFGF–LPs–pEGFP complexes (in the quantity required to deliver 2 μg DNA per well), which were composed of DNA/liposomes (weight ratio, 1:5). After 4 h incubated at 37 °C under 5% CO_2, the medium was removed and cells were incubated with complete DMEM for 24 h. GFP expression was visualized by light microscopy and assessed by fluorescent microscopy (ESP Elite, Beckman-Coulter, Miami, FL).

2.6. Antiproliferative activity in vitro

Antiproliferative activity of tbFGF–LPs–DOX–MsurvivinT34A, tbFGF–LPs–DOX, LPs–DOX and DOX was measured in MTT assay. Cells (LLC) were seeded in 96-well plates at a density of 1×10^5/ml (0.1 ml of medium per well), and exposed to respectively liposomes or DOX. The concentration of free DOX or DOX encapsulated in liposomes was 5, 2.5, 1.25, 0.625 and 0.3125 μg/ml. The control group was treated with LPs contained equivalent dose of cationic liposomes as LPs–DOX and 6 wells were left as blank. After 48 h 20 μl MTT was added to each well and the absorbance was measured at 570 nm 3 h later by the Spectramax M5 Microtiter Plate Luminometer (Molecular Device, USA) (Shi et al., 2009).

2.7. Flow cytometry and apoptosis analysis

LLC were seeded in 6-well plate and treated with 1.25 μg/ml tbFGF–LPs–DOX, tbFGF–LPs–DOX–MsurvivinT34A and DOX, at the time LPs contained equivalent dose of cationic liposomes as LPs–DOX was used as the control group. After 48 h cells were collected, washed with PBS and suspended in 1 ml hypotonic fluorochrome solution which contained 50 μg propidium iodide/ml in 0.1% sodium citrate plus 0.1% Triton X-100. The cells were analyzed by flow cytometer (ESP Elite, Beckman-Coulter, Miami, FL). Apoptotic cells appeared in the cell cycle distribution were estimated with Listmode software.

2.8. Animals and tumor model

The LLC bearing-tumor model was established in C57BL/6N mice (female; 18–20 g body weight; 8 weeks old). These mice were inoculated s.c. in the right posterior limb area with LLC (1×10^6). All these mice were purchased from Sichuan University Animal Center (Chengdu, China). All animals used in the experiments were treated humanely in accordance with Institutional Animal Care and Use Committee guidelines.

2.9. Anti-tumor activity in vivo

Tumor-bearing mice (tumor size about 5 mm × 5 mm) were divided into five groups ($n = 8$). Treatments consisted of tbFGF–LPs–DOX, tbFGF–LPs–MsurvivinT34A, tbFGF–LPs–DOX–MsurvivinT34A and control included DOX and NS. All of these groups were injected via tail vein. The dose of DOX was 2.5 mg/kg and that of Msurvivin T34A plasmid was 5 μg per mouse. All of these groups were treated on days 0, 3, 6, 9, 12 and 15. Survival time and tumor volumes were observed. Tumor size was determined by measuring of the largest and perpendicular diameters every 3 days. Tumor volumes were calculated according to the formula $V = a \times b^2 \times 0.52$, where a is the largest superficial diameter and b is the smallest superficial diameter. To detect necrosis, apoptosis and the microvessel density, tumors tissues excised were fixed in 10% formalin.

2.10. Immunohistochemistry for microvessel, cell apoptosis and proliferation analysis

Tumor tissues were fixed in 10% neutral buffered formalin solution and embedded in paraffin. The activity of inducing apoptosis was evaluated by TUNEL assay using an in situ cell death detection kit (Roche Molecular Biochemicals) following the manufacturer's protocol (Sawant and Torchilin, 2009). Cells undergoing apoptosis and necrosis were identified per high-power field. Anti-angiogenesis of every kind of liposomes and DOX were detected by paraffin sections. The paraffin sections were deparaffinized in xylol and rehydrated in graded alcohol series. Antigen retrieval was carried out by autoclaving sections in retrieval buffer (10 mM, pH 6.0 EDTA citrate buffer) for 3 min in saturated steam after up-pressure gaining (126 °C, 1.6 bars, 23 psi). Endogenous peroxidase activity was blocked by incubation in 3% hydrogen peroxide at room temperature free of light for 20 min. Nonspecific binding of reagents was quenched by incubation of sections for 20 min in 5% normal rabbit serum. Then the sections were incubated with a monoclonal rat anti-mouse CD31 overnight at 4 °C, followed by incubating with the secondary antibody, biotinylated goat anti-rat antibody. The sections were then stained with labeled streptavidin biotin reagents. Vessel density was determined by counting the number of microvessels per high-power field in the sections.

2.11. Statistical analysis

Statistical comparisons were made with one-factor analysis of variance (ANOVA). For the survival time of animals, Kaplan–Meier curves were established for each group, and the survivals were compared by means of the log rank test. Differences between means or ranks as appropriate were considered significant when yielding a $P < 0.05$. Results are presented as mean ± SD. Experiments were performed at least in triplicate.

Table 1
Mean diameter and ζ potential of liposomes.

Liposomes	Diameter (nm)	ζ Potential (mV)
LPs	87.2 ± 5	58.7 ± 8
tbFGF–LPs	164.5 ± 12	16.3 ± 10
tbFGF–LPs–DOX	285.4 ± 20	28 ± 6
tbFGF–LPs–MsurvivinT34A	498.1 ± 25	15.2 ± 5
tbFGF–LPs–DOX–MsurvivinT34A	524.7 ± 32	10.3 ± 3

3. Results and discussion

3.1. Liposome characterization

Table 1 shows the particle size and surface charge of various types of liposomes. The mean diameter of LPs, tbFGF–LPs and tbFGF–LPs–DOX were 87.2 ± 5 nm, 164.5 ± 12 nm and 285.4 ± 20 nm (mean ± SD, $n = 6$), respectively. Moreover, liposomes have larger particle size after incubating with the plasmid, the particle size of tbFGF–LPs–MsurvivinT34A and tbFGF–LPs–DOX–MsurvivinT34A were 498.1 ± 25 nm and 524.7 ± 32 nm (mean ± SD, $n = 6$). The size of LPS and tbFGF–LPs increased after DOX entrapping showed that free DOX was encapsulated. Meanwhile, after the tbFGF–LPs–DOX and Msurvivin T34A plasmid complexes forming, the size also increased. These data demonstrated that the plasmid was combined to the cationic liposome. The ζ potential of LPs, tbFGF–LPs, tbFGF–LPs–DOX, tbFGF–LPs–MsurvivinT34A and tbFGF–LPstbFGF–LPs–DOX–MsurvivinT34A were about 58.7 ± 8 mV, 16.3 ± 10 mV, 28 ± 6 mV, 5.2 ± 5 mV and 10.3 ± 3 mV (mean ± SD, $n = 6$). The surface charge decreasing after mixing of tbFGF–LPs and tbFGF–LPs–DOX with MsurvivinT34A plasmid may be owing to the electrostatic interactions between lipids and plasmid.

3.2. Transfection in vitro

The results of the LLC treated with LPs–pEGFP and tbFGF–LPs–pEGFP complexes were presented in Fig. 1. The flow cytometry data (Fig. 1B) showed the transfection efficiency of the treatment of LLC with LPs–pEGFP was only 3.4 ± 0.09%. At similar conditions, cells treated with tbFGF–LPs–pEGFP complexes demonstrated a higher fluorescence, which was 9.3 ± 0.15%. These results suggest that the plain cationic liposome have obtained the higher efficient transfection through combining with the tbFGF. The transfection efficiency were expressed as mean ± SD, $n = 3$.

3.3. Antiproliferative activity

Antiproliferative activity of DOX and various kinds of liposomes against LLC was evaluated by MTT assay. The antiproliferative activity of DOX and various kinds of liposomes was shown in Fig. 2. LLC were exposed to various concentrations of DOX, LPs–DOX, tbFGF–LPs–DOX and tbFGF–LPs–DOX–MsurvivinT34A, respectively. The antiproliferative activity of tbFGF–LPs–DOX–MsurvivinT34A was the highest in all of the groups, with the IC_{50} value of 1.8 ± 0.08 μM (Table 2).

Table 2
Antiproliferatve activity of DOX and various kinds of liposomes against LLC *in vitro*.

Liposomes	IC_{50}[a]
DOX	3.6 ± 0.10 μM
LPs–DOX	5.3 ± 0.11 μM
tbFGF–LPs–DOX	2.2 ± 0.06 μM
tbFGF–LPs–DOX–MsurvivinT34A	1.8 ± 0.08 μM

[a] 50% inhibitory concentration.

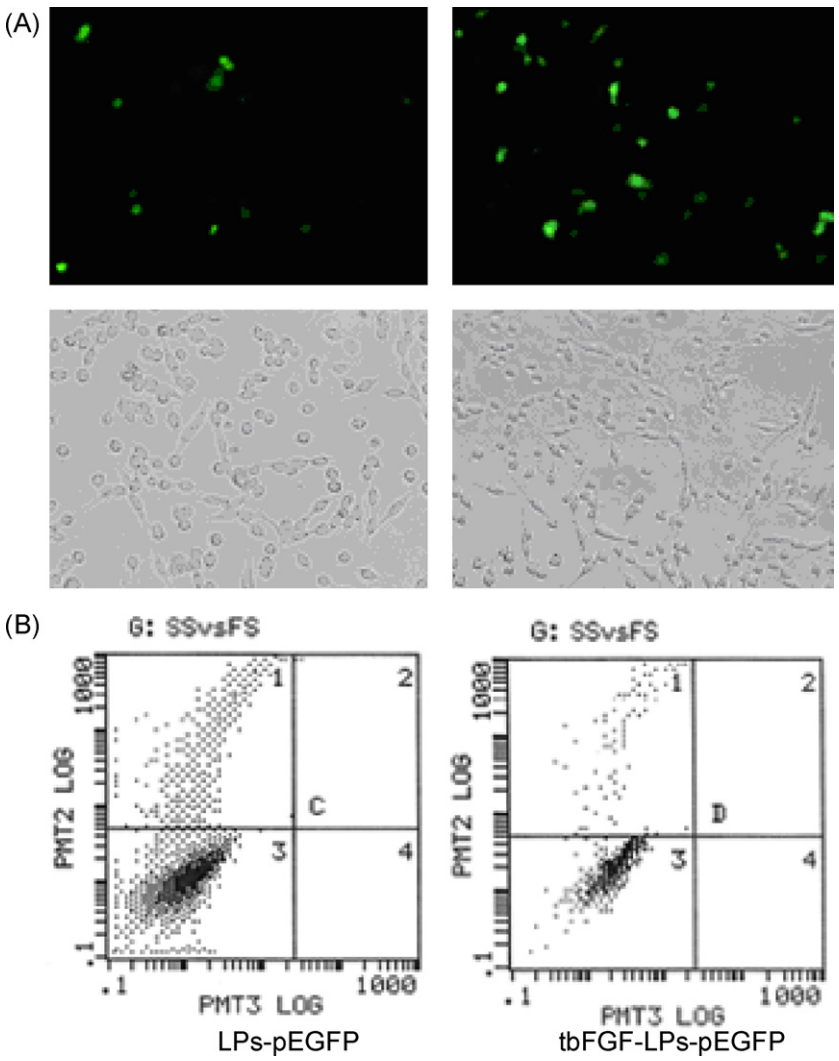

Fig. 1. (A) Images show the plain cationic liposomes combining tbFGF increase transfection in LLC. (B) Flow cytometry analysis of the effects of LPs–pEGFP, tbFGF–LPs–pEGFP complexes in LLC. The liposomes–pEGFP complexes were composed of DNA/liposomes (weight ratio, 1:5).

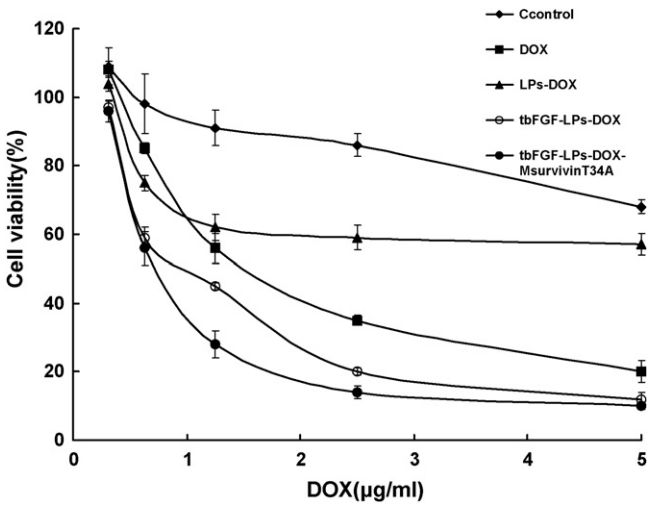

Fig. 2. Antiproliferative activity of various kinds of lipsomes exposured in LLC. LLC were treated with tbFGF–LPs–DOX–MsurvivinT34A, tbFGF–LPs–DOX, LPs–DOX and DOX at concentration of 5, 2.5, 1.25, 0.625, 0.3125 μg/ml and LPs as the control group contained equivalent dose of cationic liposomes as LPs–DOX. After 48 h, cell viability was quantified by a standard MTT assay. ♦ Control; ■ DOX; ▲ LPs–DOX; ○ tbFGF-LPs–DOX; ● tbFGF–LPstbFGF–LPs–DOX–MsurvivinT34A.

This result could suggest that the synergistic/combined effect has been achieved by tbFGF–LPs as an efficacy vector to co-deliver the drug and gene to the same cells *in vitro*. Meanwhile, the DOX had a slightly lower IC_{50} value of 3.6 ± 0.10 μM compared to 5.3 ± 0.11 μM of LPs–DOX, which was probably a result of sequestration of the drug within the liposomes leading to low amounts of drug released from the liposomes and taken up by cells. However, IC_{50} value for tbFGF–LPs–DOX is 2.2 ± 0.06 μM that was lower than free DOX. This enhanced antiproliferative activity may contribute to the fact that this tbFGF-modified cationic liposome could improve tumor specific attachment to cancer cells, resulting in enhancing drugs uptaken by cells (Table 2). The IC_{50} values were expressed as mean ± SD, $n = 4$.

3.4. Flow cytometry analysis

Apoptosis was measured by sub-G1 DNA content determined by flow cytometry. The cells in sub-G1 phase were considered as apoptotic cells. The apoptosis rate in LPs, 1.25 μg/ml DOX and tbFGF–LPs–DOX were $6.1 \pm 1.2\%$, $14.3 \pm 2.4\%$, and $23.6 \pm 1.5\%$, respectively. The apoptosis rate in co-delivery treatment was $32.3 \pm 4.2\%$, which was the highest in all the groups (Fig. 3). These results further supported that this novel cationic liposome designed by our lab could lead to specifically locate in

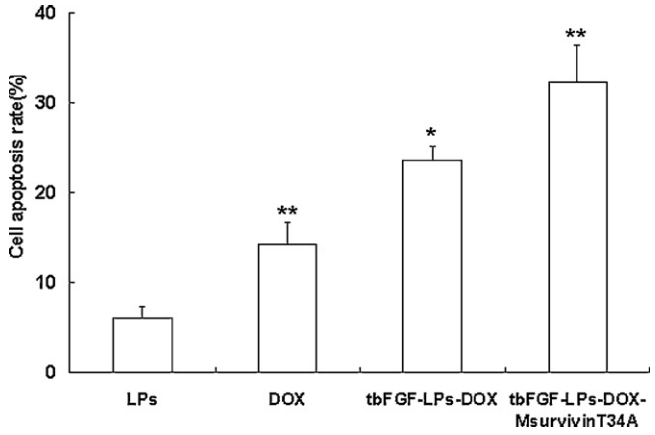

Fig. 3. Apoptosis effect of various kinds of lipsomes exposured in LLC. LLC were treated with 1.25 μg/ml tbFGF-LPs–DOX, tbFGF–LPstbFGF–LPs–DOX–MsurvivinT34A, DOX and LPs as the control group contained equivalent dose of cationic liposomes as LPs–DOX. After 48 h, the cells were analyzed by flow cytometer. The data shows the apoptosis rate (mean ± SD). $^{*}P < 0.05$, $^{**}P < 0.01$.

tumors and result in uptaken by cells increasing. Moreover, it also demonstrated that the novel liposome as a vector co-delivering drugs and plasmid in same cells *in vitro* was successfully because the highest apoptosis rate obtained as cells treated by tbFGF–LPs–DOX–MsurvivinT34A.

3.5. Anti-tumor effect of the co-delivering system in vivo

In order to demonstrate the synergistic/combined effect of co-delivery system *in vivo*, Msurvivin T34A plasmid was used as a therapeutic gene to be co-delivered with DOX into LLC bearing C57BL/6N mice by injecting via tail vein. On days18 after treatment, as shown in Fig. 4B, the tumor volume in the mice treated with tbFGF–LPs–DOX–MsurvivinT34A was 983 ± 136 mm^3 with 80% decrease compared to that of untreated tumor volume, while the tbFGF–LPs–DOX, tbFGF–LPs–MsurvivinT34A and DOX only reduced the tumor volume by 70% (1485 ± 184 mm^3), 41% (2952 ± 209 mm^3) and 67% (1630 ± 202 mm^3) respectively as compared to the NS groups (4951 ± 164 mm^3). Meanwhile, the treatment by Msurvivin T34A plasmid co-delivered with DOX significantly resulted in improving the survival time versus the other groups (Fig. 4C). The tbFGF–LPs–DOX–MsurvivinT34A has resulted in longer than 15 days delay of tumor growth to reach 4000 mm^3. In contrast, tbFGF–LPs–DOX, tbFGF–LPs–MsurvivinT34A and DOX only led to 9, 6 and 6 days delay of tumor growth to reach 4000 mm^3. The delay time of tumor growth was defined as the different time of tumor volume reached 4000 mm^3 in average between treated groups and control group. All of these results indicated that a significant synergistic/combined effect of co-delivering of DOX and Msurvivin T34A plasmid have been gained *in vivo* by using this novel cationic liposome. The tumor volumes were expressed as mean ± SD, $n = 8$.

3.6. Synergistic/combined induction of apoptosis

DNA fragmentation by TUNEL detection revealed the different activities of inducing apoptosis in all the groups. Treatment with tbFGF–LPs–DOX, tbFGF–LPs–MsurvivinT34A and DOX increased apoptosis compared to the untreated group. What is more, the tbFGF–LPs–DOX–MsurvivinT34A induced the highest apoptosis in all the groups. As shown in Fig. 5, significant increases of TUNEL-positive nuclei were found in the co-delivering system compared to the tbFGF–LPs–DOX, tbFGF–LPs–MsurvivinT34A and DOX. These data supposed that drugs and plasmid or plasmid and plasmid even drugs and drugs could be administered to animals or humans

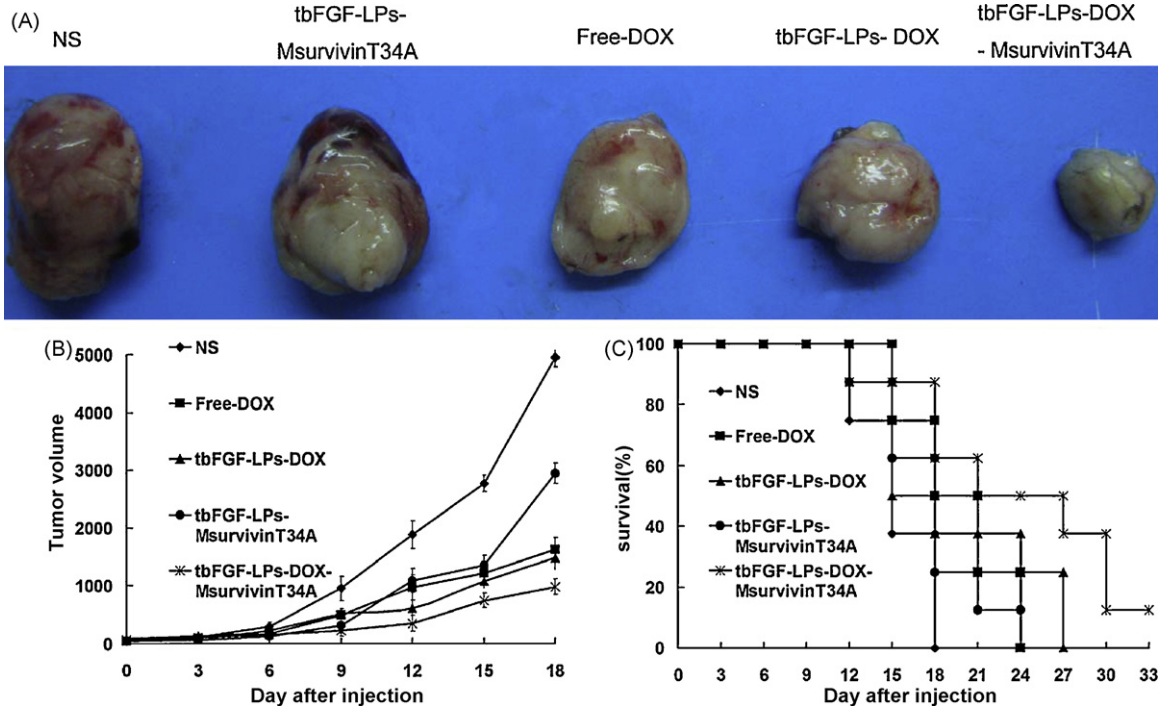

Fig. 4. Anti-tumor effect of DOX, tbFGF-LPs–DOX, tbFGF–LPstbFGF–LPs–MsurvivinT34A, tbFGF-LPs–DOX–MsurvivinT34A *in vivo*. (B) Tumor growth after being treated with DOX, tbFGF–LPs–DOX, tbFGF–LPs–MsurvivinT34A, tbFGF–LPs–DOX–MsurvivinT34A and NS in a Lewis lung carcinoma model. Eight mice per group were used. Data were presented as mean ± SD. (C) Survival curves of C57BL/6N mice bearing Lewis lung carcinoma treated with DOX, tbFGF–LPs–DOX, tbFGF–LPs–MsurvivinT34A., tbFGF–LPs–DOX–MsurvivinT34A and NS. LLC (1×10^6/mice, 8 mice/group) were inoculated s.c in the right flank. Treatment was administered i.v. as tumor size about 5 mm × 5 mm on day 0.

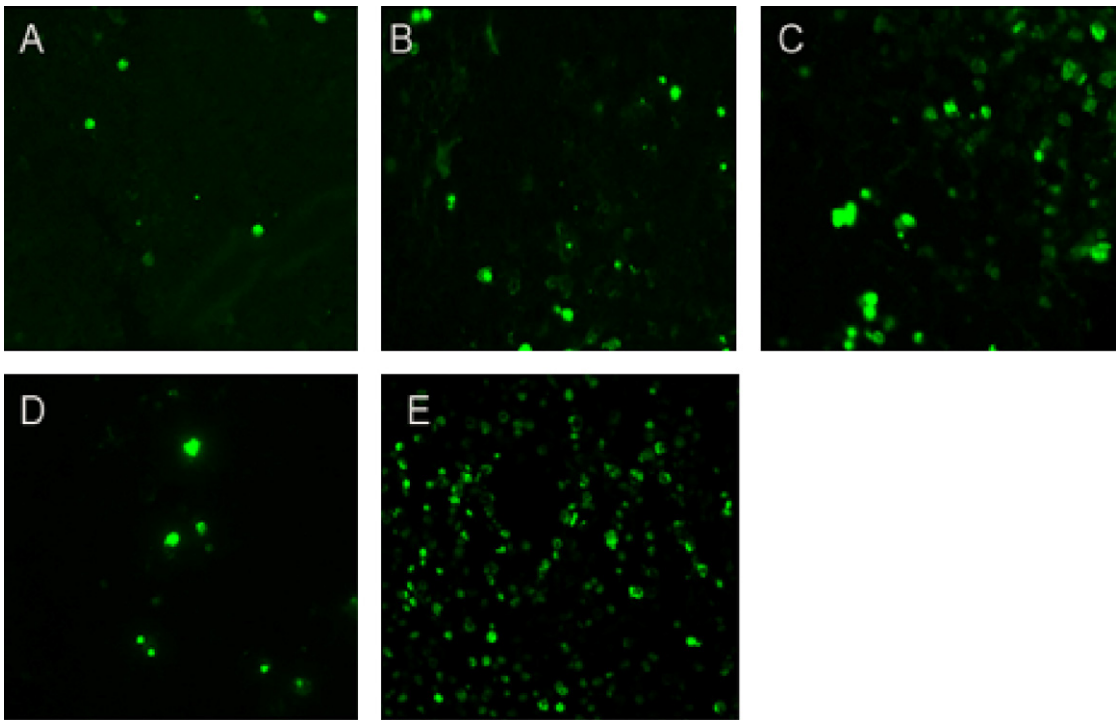

Fig. 5. Terminal deoxynucleotidyltransferase-mediated dUTP nick-end labeling staining of tumor tissues. Sections after treatment were stained by TUNEL analysis to detect apoptotic cells (400×). (A) NS, (B) DOX, (C) tbFGF–LPs–DOX, (D) tbFGF–LPs–MsurvivinT34A and (E) tbFGF–LPs–DOX–MsurvivinT34A.

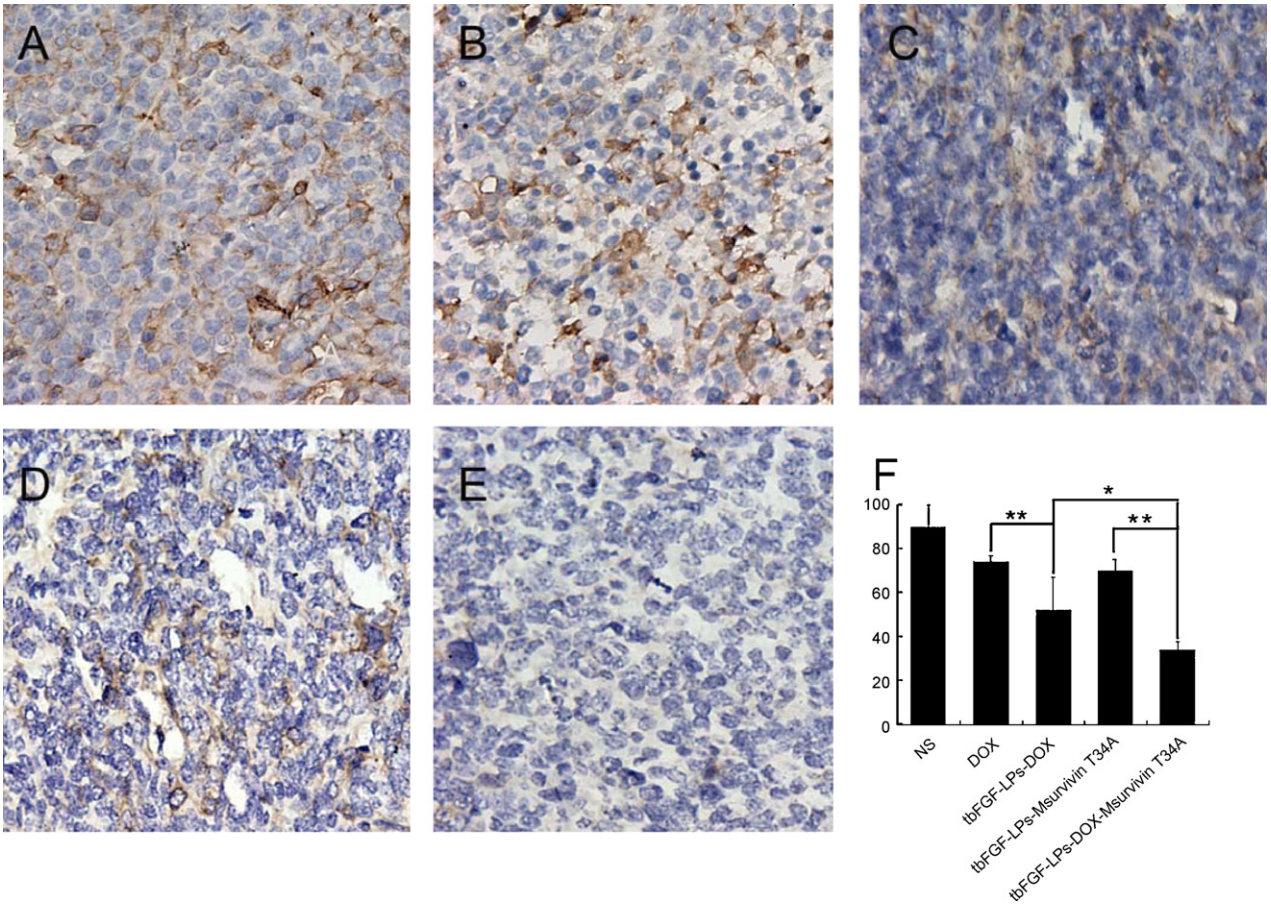

Fig. 6. Immunohistochemical analysis of CD31 protein levels as a marker of vascular cells. Vascularization with tumors was detected by an antibody CD31 and vascular density was quantified by counting the number of microvessel per field (400×). (A) NS, (B) DOX, (C) tbFGF–LPs–DOX, (D) tbFGF-LPs–MsurvivinT34A, (E) tbFGF–LPs–DOX–MsurvivinT34A and (F) CD31 positive microvessel in each group. Values were expressed as mean ± SD $^{*}P < 0.05$, $^{**}P < 0.01$.

only by one appropriate vector and synergistic/combined effect were obtained. This hypothesis led to the number of injections reduced, which may result in compliance increasing in clinical treatment.

3.7. Synergistic/combined inhibition of angiogenesis

Angiogenesis within tumor tissue was estimated in tumor sections stained with an antibody reactive to CD31 and quantified as described in Section 2. Compared to untreated group, tbFGF–LPs–DOX, tbFGF–LPs–MsurvivinT34A and DOX led to apparent inhibition of angiogenesis in tumors. The average number of blood vessels observed at a magnification of 400× in tumors treated with NS, DOX, tbFGF–LPs–DOXLPs–DOX, tbFGF–LPs–MsurvivinT34A and tbFGF–LPs–DOX–MsurvivinT34A were 90.13 ± 9.6, 74.58 ± 2.9, 51.18 ± 15.0, 70.63 ± 5.4 and 34 ± 3.6 (Fig. 6F). Reduced numbers of blood vessels in tumors treated with tbFGF–LPs–DOX–MsurvivinT34A in comparison with tbFGF–LPs–DOX ($P = 0.024$), tbFGF–LPs–MsurvivinT34A ($P = 0.001$), tbFGF–LPs–DOX and DOX ($P = 0.002$) so significantly suggested that the more reduction of tumor visualization may contribute to enhance tumor regression. This data further illustrated the advantage of the novel delivery system *in vivo*.

3.8. Toxicity assays

During the experiment all groups of mice were well tolerated towards DOX and no gross signs of cumulative adverse consequences were observed such as huddling, weight loss, ruffling of fur, life span, behavior, and feeding. Furthermore, no pathologic changes in liver, lung, kidney, spleens, brain, heart, pancreas, intestines, or bone marrow were found by microscopic examination. In order to measure systemic toxicity of the treatments, pathologic inspection was assessed by hematoxylin and eosin staining of sections. No pathologic changes in liver, lung, kidney, spleens, brain, heart, pancreas, intestines, or bone marrow were found by microscopic examination (data not shown).

4. Conclusion

The data presented in this report confirmed our hypothesis that this tbFGF-modified cationic liposome can be used as the vector co-delivering drugs and gene to gain the synergistic/combined effect after improving the transfection efficacy by combining with tbFGF. Our study reveals the perspective of this liposome as a novel delivery system. The Msurvivin T34A plasmid can be replaced with synthetic siRNA or another DNA and they can be successfully co-delivered with drugs to enhance gene expression or to achieve the synergistic/combined effect in gene therapy. Meanwhile, this co-delivery system may provide a new treatment strategy for tumors.

Acknowledgement

This work was supported by National 863 Program (2007AA021201) of China.

References

Asanuma, K., Moriai, R., Yajima, T., Yagihashi, A., Yamada, M., Kobayashi, D., Watanabe, N., 2000. Survivin as a radioresistance factor in pancreatic cancer. Jpn. J. Cancer Res. 91, 1204–1209.

Batist, G., Ramakrishnan, G., Rao, C.S., Chandrasekharan, A., Gutheil, J., Guthrie, T., Shah, P., Khojasteh, A., Nair, M.K., Hoelzer, K., Tkaczuk, K., Park, Y.C., Lee, L.W., 2001. Reduced cardiotoxicity and preserved antitumor efficacy of liposome-encapsulated doxorubicin and cyclophosphamide compared with conventional doxorubicin and cyclophosphamide in a randomized, multicenter trial of metastatic breast cancer. J. Clin. Oncol. 19, 1444–1454.

Chen, X., Wang, X.H., Wang, Y.S., Yang, L., Hu, J., Xiao, W.J., Fu, A.F., Cai, L.L., Li, X., Ye, X., Liu, Y.L., Wu, W.S., Shao, X.M., Mao, Y.Q., Wei, Y.Q., Chen, L.J., 2010. Improved tumor-targeting drug delivery and therapeutic efficacy by cationic liposome modified with truncated bFGF peptide. J. Control Release, doi:10.1016/j.jconrel.2010.03.007.

Ghera, B.B., Perret, F., Chevalier, Y., Parrot-Lopez, H., 2009. Novel nanoparticles made from amphiphilic perfluoroalkyl α-cyclodextrin derivatives: Preparation, characterization and application to the transport of acyclovir. Int. J. Pharm. 375, 155–162.

Grossman, D., Kim, P.J., Schechner, J.S., Altieri, D.C., 2001. Inhibition of melanoma tumor growth in vivo by survivin targeting. Proc. Natl. Acad. Sci. USA 98, 635–640.

Gu, D.L., Gonzalez, A.M., Printz, M.A., Doukas, J., Ying, W., D'Andrea, M., Hoganson, D.K., Curiel, D.T., Douglas, J.T., Sosnowski, B.A., Baird, A., Aukerman, S.L., Pierce, G.F., 1999. Fibroblast growth factor 2 retargeted adenovirus has redirected cellular tropism: evidence for reduced toxicity and enhanced antitumor activity in mice. Cancer Res. 59, 2608–2614.

Hara, T., Aramaki, Y., Takada, S., Koike, K., Tsuchiya, S., 1995. Receptor-mediated transfer of pSV2CAT DNA to a human hepatoblastoma cell line HepG2 using asialofetuin-labeled cationic liposomes. Gene 159, 167–174.

Henk, J.B., Kristy, J.G., Henk, M.W.V., 2009. Understanding the causes of multidrug resistance in cancer: a comparison of doxorubicin and sunitinib. Drug Resist Update 12, 114–126.

Janát-Amsbury, M.M., Yockman, J.W., Lee, M., Kern, S., Furgeson, D.Y., Bikram, M., Kim, S.W., 2004. Combination of local, nonviral IL12 gene therapy and systemic paclitaxel treatment in a metastatic breast cancer model. Mol. Ther. 9, 829–836.

Kanwar, J.R., Shenm, W.P., Kanwar, R.K., Berg, R.W., Krissansen, G.W., 2001. Effects of survivin antagonists on growth of established tumors and B7-1 immunogene therapy. J. Natl. Cancer Inst. 93, 1541–1552.

Kishida, T., Asada, H., Itokawa, Y., Yasutomi, K., Shin-Ya, M., Gojo, S., Cui, F., Ueda, Y., Yamagishi, H., Imanishi, J., Mazda, O., 2003. Electrochemo-gene therapy of cancer: intratumoral delivery of interleukin-12 gene and bleomycin synergistically induced therapeutic immunity and suppressed subcutaneous andmetastatic melanomas in mice. Mol. Ther. 8, 738–745.

Kleeff, J., Fukahi, K., Lopez, M.E., Friess, H., Buchler, M.W., Sosnowski, B.A., Korc, M., 2002. Targeting of suicide gene delivery in pancreatic cancer cells via FGF receptors. Cancer Gene Ther. 9, 522–532.

Liu, F., Shollenberger, L.M., Huang, L., 2004. Non-immunostimulatory nonviral vectors. FASEB J. 18, 1779–1781.

Nakase, M., Inui, M., Okumura, K., Kamei, T., Nakamura, S., Tagawa, T., 2005. p53 gene therapy of human osteosarcoma using a transferrin-modified cationic liposome. Mol. Cancer Ther. 4, 625–631.

Paduano, F., Villa, R., Pennati, M., Folini, M., Binda, M., Daidone, M.G., Zaffaron, N., 2006. Silencing of survivin gene by small interfering RNAs produces supra-additive growth suppression in combination with 17-allylamino-17-demethoxygeldanamycin in human prostate cancer cells. Mol. Cancer Ther. 5, 179–186.

Peng, X.C., Yang, L., Yang, L.P., Mao, Y.Q., Yang, H.S., Liu, J.Y., Zhang, D.M., Chen, L.J., Wei, Y.Q., 2008. Efficient inhibition of murine breast cancer growth and metastasis by gene transferred mouse survivin Thr34→Ala mutant. J. Exp. Clin. Cancer Res. 27, 46–58.

Printz, M.A., Gonzalez, A.M., Cunningham, M., Gu, D.L., Ong, M., Pierce, G.F., Aukerman, S.L., 2000. Fibroblast growth factor 2-retargeted adenoviral vectors exhibit a modified biolocalization pattern and display reduced toxicity relative to native adenoviral vectors. Hum. Gene Ther. 11, 191–204.

Rancourt, C., Rogers, B.E., Sosnowski, B.A., Wang, M., Piche, A., Pierce, G.F., Alvarez, R.D., Siegal, G.P., Douglas, J.T., Curiel, D.T., 1998. Basic fibroblast growth factor enhancement of adenovirus-mediated delivery of the herpes simplex virus thymidine kinase gene results in augmented therapeutic benefit in a murine model of ovarian cancer. Clin. Cancer Res. 4, 2455–2461.

Rogers, B., Douglas, J., Ahlem, C., Buchsbaum, D., Frincke, J., Curiel, D., 1997. Use of a novel cross-linking method to modify adenovirus tropism. Gene Ther. 4, 1387–1392.

Salvesen, G.S., Duckett, C.S., 2002. Apoptosis: IAP proteins: blocking the road to death's door. Nat. Rev. Mol. Cell Biol. 3, 401–410.

Sawant, R.R., Torchilin, V.P., 2009. Enhanced cytotoxicity of TATp-bearing paclitaxel-loaded micelles *in vitro* and *in vivo*. Int. J. Pharm. 374, 114–118.

Shi, P.J., Zuo, Y., Qin, Z., Shen, J., Zhang, L., Li, Z., Li, Y.B., Morsi, Y.S., 2009. Improved properties of incorporated chitosan film with ethyl cellulose microspheres for controlled release. Int. J. Pharm. 375, 67–74.

Takanami, I., Imamuma, T., Hashizume, T., Kikuchi, K., Yamamoto, Y., Yamamoto, T., Kodaira, S., 1996. Expression of PDGF IGF-II, bFGF and TGF-beta1 in pulmonary adenocarcinoma. Pathol. Res. Pract. 192, 1113–1120.

Tan, C., Etcuhanas, E., Wollner, N., Rosen, G., Gilladoga, A., Showel, J., Murphy, M.L., Krakoff, I.H., 1973. Adriamycin-an antitumor antibiotic in the treatment of neoplastic disease. Cancer (Phila.) 32, 9–17.

Thurston, G., McLean, J.W., Rizen, M., Baluk, P., Haskell, A., Murphy, T.J., Hanahan, D., McDonald, D.M., 1998. Cationic liposomes target angiogenic endothelial cells in tumors and chronic inflammation in mice. J. Clin. Investig. 101, 1401–1413.

Van Heeswijk, W.A.R., Stoffer, T., Eenick, M.J.D., Potman, W., Van der Vijgh, W.J.F., Van der Poort, J., Pinedo, H.M., Lelieveld, P., Feijen, J., 1984. Synthesis, characterization and antitumor activity of macromolecular prodrugs of adriamycin.

In: Anderson, J.M., Kim, S.W. (Eds.), Recent Advances in Drug Delivery Systems. Plenum, New York, pp. 77–100.
Volm, M., Koomagi, R., Mattern, J., Stammler, G., 1997. Angiogenic growth factors and their receptors in non-small cell lung carcinomas and their relation shis to drug response in vitro. Anticancer Res. 17, 99–103.
Xu, M., Kumar, D., Srinivas, S., Detolla, L.J., Yu, S.F., Stass, S.A., Mixson, A.J., 1997. Parenteral gene therapy with p53 inhibits human breast tumor *in vivo* through a bystander mechanism without evidence of toxicity. Hum. Gene Ther. 8, 177–185.
Zhang, X., Collins, L., Sawyer, G.J., Dong, X., Qiu, Y., Fabre, J.W., 2001. *In vivo* gene delivery via portal vein and bile duct to individual lobes of the rat liver using a polylysine-based nonviral DNA vector in combination with chloroquine. Hum. Gene Ther. 12, 2179–2190.
Zou, Y.Y., Ling, Y.H., Van, N.T., Priebe, W., Perez-Soler, R., 1994. Antitumor activity of free and liposome-entrapped annamycin, a lipophilic anthracycline antibiotic with non-cross-resistance properties. Cancer Res. 54, 1479–2148.